Am J Physiol Renal Physiol 304: F1217–F1229, 2013.
First published March 6, 2013; doi:10.1152/ajprenal.00070.2013.

A method to facilitate and monitor expression of exogenous genes in the rat kidney using plasmid and viral vectors

Peter R. Corridon,[1,2] George J. Rhodes,[2] Ellen C. Leonard,[3] David P. Basile,[3] Vincent H. Gattone II,[4] Robert L. Bacallao,[2,5]* and Simon J. Atkinson[1,2,6]*

[1]*Biomolecular Imaging and Biophysics Graduate Program, Indiana University School of Medicine, Indianapolis, Indiana;* [2]*Division of Nephrology, Department of Medicine, Indiana University School of Medicine, Indianapolis, Indiana;* [3]*Department of Cellular and Integrative Physiology, Indiana University School of Medicine, Indianapolis, Indiana;* [4]*Department of Anatomy and Cell Biology, Indiana University School of Medicine, Indianapolis, Indiana;* [5]*Richard, L. Roudebush Veterans Affairs Medical Center, Indianapolis Indiana; and* [6]*Department of Biology, Indiana University-Purdue University, Indianapolis, Indiana*

Submitted 4 February 2013; accepted in final form 28 February 2013

Corridon PR, Rhodes GJ, Leonard EC, Basile DP, Gattone VH II, Bacallao RL, Atkinson SJ. A method to facilitate and monitor expression of exogenous genes in the rat kidney using plasmid and viral vectors. *Am J Physiol Renal Physiol* 304: F1217–F1229, 2013. First published March 6, 2013; doi:10.1152/ajprenal.00070.2013.—Gene therapy has been proposed as a novel alternative to treat kidney disease. This goal has been hindered by the inability to reliably deliver transgenes to target cells throughout the kidney, while minimizing injury. Since hydrodynamic forces have previously shown promising results, we optimized this approach and designed a method that utilizes retrograde renal vein injections to facilitate transgene expression in rat kidneys. We show, using intravital fluorescence two-photon microscopy, that fluorescent albumin and dextrans injected into the renal vein under defined conditions of hydrodynamic pressure distribute broadly throughout the kidney in live animals. We found injection parameters that result in no kidney injury as determined by intravital microscopy, histology, and serum creatinine measurements. Plasmids, baculovirus, and adenovirus vectors, designed to express EGFP, EGFP-actin, EGFP-occludin, EGFP-tubulin, tdTomato-H2B, or RFP-actin fusion proteins, were introduced into live kidneys in a similar fashion. Gene expression was then observed in live and ex vivo kidneys using two-photon imaging and confocal laser scanning microscopy. We recorded widespread fluorescent protein expression lasting more than 1 mo after introduction of transgenes. Plasmid and adenovirus vectors provided gene transfer efficiencies ranging from 50 to 90%, compared with 10–50% using baculovirus. Using plasmids and adenovirus, fluorescent protein expression was observed *1*) in proximal and distal tubule epithelial cells; *2*) within glomeruli; and *3*) within the peritubular interstitium. In isolated kidneys, fluorescent protein expression was observed from the cortex to the papilla. These results provide a robust approach for gene delivery and the study of protein function in live mammal kidneys.

hydrodynamic plasmid and adenovirus transgene delivery; fluorescent protein expression in kidney cortex and medulla; intravital two-photon fluorescence microscopy; confocal laser scanning microscopy

RELIABLE METHODS FOR GENE transfer to specific target cells in live animals have the potential both to enhance basic and disease-focused research in animal models and to facilitate the advancement of gene therapy in humans. Numerous methods have been proposed to deliver exogenous genes to mammalian cells in situ (4, 6, 12, 14, 19). These techniques could provide inexpensive and rapid alternatives to pronuclear microinjection-derived transgenic models (13). However, more efficient approaches are needed to enhance gene transfer by improving the distribution, extent, and duration of gene expression, while minimizing injury associated with the delivery.

Generally, in vivo gene transfer success is directly influenced by the following phenomena: *1*) the ability to deliver vectors to the target cell; *2*) the time taken for cells to express the delivered genes; *3*) the number of cells that incorporate the exogenous genes; *4*) the level of the resulting expression; *5*) cellular turnover rates; *6*) reproducibility of the process; and *7*) the extent and severity of any injury that may result from the gene delivery process (27).

Efficient gene transfer has been difficult to achieve routinely in the kidney (21, 27), as illustrated by the varied levels of successful transgene incorporation reported in previous studies (35, 42), and more generally, the failure of any of these methods to achieve widespread use. The structure of various renal vascular beds and their permeability characteristics present intrinsic challenges to gene transfer processes. For example, proximal tubule epithelial cells have an immense capacity for the apical endocytic uptake of exogenous materials, and thus the possibility of transgene incorporation (9, 21, 27, 35, 42). Yet, the accessibility of the apical domain to exogenously delivered vectors, and accordingly the resulting extent of transgene uptake, are strongly limited by the permeability characteristics of the glomerular filtration barrier (21). The degree to which proximal tubule cells are accessible for gene delivery at the basolateral surface, via the peritubular capillaries, is largely unknown.

Adenoviral vectors have been widely used for transgene expression in other organs (12, 15, 18, 28, 34). In the kidney, however, previous studies have observed widely varying levels of gene expression using adenovirus vectors. In those studies, the adenoviral vectors were delivered through arterial injections in normal (35, 48, 50) and cystic (50) rats; via pelvic catheter infusion in normal rats (50); and via tail vein (42) and cortical micropuncture (41) injections in uninjured animals. These studies differ considerably in the cell types and anatomic regions of the kidney in which gene expression was detected, and in the pervasiveness of expression across the organ. While some of these differences may be accounted for by the particular genes being expressed or by features of the vector system, a more significant factor is probably found in the delivery route or the existence of underlying disease processes that would

*R. L. Bacallao and S. J. Atkinson contributed equally to this work.

Address for reprint requests and other correspondence: S. J. Atkinson, Dept. of Biology, Indiana Univ.-Purdue Univ. Indianapolis, 723 West Michigan St., SL 306B, Indianapolis, IN 46202 (e-mail: satkinso@iupui.edu).

alter kidney microanatomy. Collectively, these results point to the importance of anatomic obstacles influencing the pattern of transgene expression from these vectors.

Others have explored direct transfer of adenovirus vectors into individual nephron segments using micropuncture techniques, achieving site-specific genetic incorporation within the injected tubules or vascular welling points (41). One limitation of the approach, however, is that gene expression is restricted to the injection site. There is also a risk of injury from transgene delivery via inflammatory responses generated from large concentrations of adenovirus vectors. Importantly, this result also demonstrated the utility of intravital fluorescent two-photon microscopy as a means of directly monitoring protein expression in live animals.

Hydrodynamic fluid delivery has been proposed as a method for improving gene transfer rates in the kidney by increasing vascular permeability to efficiently deliver exogenous substances throughout the kidney (31). By impacting fluid pressures within thin and stretchable capillaries (37), this process is believed to increase the permeability of the capillary endothelium (37) and epithelial junctions (44), and to generate transient pores in plasma membranes facilitating the cellular internalization of macromolecules of interest (17). Systemic hydrodynamic gene delivery has been used successfully with the liver as the target organ (5, 37, 49), but renal expression has not been achieved with systemic delivery. However, the unique anatomy of the kidney provides various innate delivery paths (renal artery, renal vein, and ureter) that may be ideal for hydrodynamic gene delivery (47) directly to the organ. In particular, it has been suggested that the relatively low-pressure renal venous system would provide a feasible site for hydrodynamic injections, by facilitating exogenous transgene delivery and limiting injection-related tissue damage (38, 47). Plasmids (7, 16, 25, 30, 31, 36, 45–47, 49), baculovirus (1, 2, 23, 24, 39), and adenovirus (21, 29, 35, 41, 45) vectors have been previously identified as useful agents for in vitro and in vivo mammalian gene delivery. These vectors are reported to generate relatively low levels of pathogenicity and toxicity, are capable of carrying large DNA inserts, and can be generated in sufficiently high concentrations to provide sustained transgene expression (22, 23, 29, 30).

The aim of the present study was to develop a simplified technique to rapidly induce and monitor transgene expression in live rat kidneys, without significant accompanying injury. We utilized two-photon and confocal laser-scanning microscopy to evaluate the hydrodynamic venous delivery of transgenes using plasmids, baculovirions, and adenovirions.

MATERIALS AND METHODS

Cell Culture

Mouse kidney cell culture. We used epithelial cells from the S3 segment of proximal tubules (20). These cells were cultured in medium prepared by combining 500 ml of essential medium (Fisher Scientific, Pittsburgh, PA) with 7.5% of sodium bicarbonate, 7% of fetal bovine serum (FBS), and 1% of Pen-Strep, (Fisher Scientific). The cells were grown in a 37°C, 5% CO_2-38% O_2 humid incubator.

Madin-Darby canine kidney cell culture. Madin-Darby canine kidney (MDCK) strain II cells (43) were grown in minimal essential media (Fisher Scientific) with 8% FBS, 1% L-glutamine, penicillin/streptomycin (Fisher Scientific), and hygromycin (Calbiochem, San Diego, CA), and kept in a 37°C, 5% CO_2 humid incubator.

Rats

For these studies we used rats ranging in weight from 150 to 470 g. Male and female Sprague-Dawley, Frömter-Munich-Wistar (Harlan Laboratories, Indianapolis, IN), and Simonsen-Munich-Wistar (Simonsen's Laboratory, Gilroy, CA) rats. The Munich-Wistar rats were bred in the Indiana University School of Medicine Laboratory Animal Resource Center. The rats were given free access to standard rat chow and water throughout our studies. All experiments were conducted in accordance with National Institutes of Health guidelines and were approved by the Indiana University School of Medicine Institutional Animal Care and Use Committee.

Dyes and Fluorescent Probes

Tolonium chloride. We prepared stock solutions by dissolving 50 mg of tolonium chloride dye (Toluidine Blue O, Electron Microscopy Sciences, Fort Washington, PA), in 5 ml of 0.9% saline. For each hydrodynamic injection, 0.5 ml of this mixture was used.

Albumin, dextrans, and Hoechst. The following fluorescent probes were used in our intravital two-photon fluorescent imaging studies: Texas Red-labeled albumin in PBS prepared by combining Texas red sulfonyl chloride (Life Technologies, Carlsbad, CA) and albumin fraction V powder (Sigma-Aldrich, St. Louis, MO); 3-kDa Cascade Blue; 4- and 150-kDa FITC-dextrans (Invitrogen, Carlsbad, CA); 150-kDa tetramethyl rhodamine isothiocyanate (TRITC)-dextran (TdB Consultancy, Uppsala, Sweden); and Hoechst 33342 (Invitrogen, Carlsbad, CA). The final albumin and dextran injection solutions were prepared from diluting 50 μl of each 20 mg/ml stock solution in 0.5–1 ml of saline, and 30–50 μl of Hoechst was diluted in 0.5 ml of saline (41).

Transgene Vectors

Plasmid vectors. Plasmid DNA was isolated using Qiagen Maxi Prep systems (Qiagen, Chatsworth, CA). These plasmids encoded enhanced green fluorescent protein (EGFP), EGFP-actin, and EGFP-tubulin (Clontech Laboratories, Mountain View, CA); EGFP-occludin (a gift from Dr. Clark Wells, Indiana University School of Medicine); and H2B-tdTomato (a gift from Dr. Richard Day, Indiana University School of Medicine). For hydrodynamic injections, the range of doses we used was 1–3 μg of plasmid DNA/g of body weight diluted in 0.5 ml of saline.

Baculovirus vectors. Cellular Light GFP, EGFP-actin, and Null (control) BacMam 2.0 baculovirus expression vectors were from Life Technologies. The EGFP-actin baculovirus vector encoded fluorescent proteins with a human sequence targeting them to both filamentous and globular actin. The Null reagent lacks mammalian genetic constituents and is designed to identify potential baculovirus-mediated effects and distinguish fluorescence signals from innate tissue fluorescence. A range of doses was used, spanning 1×10^5 to 1×10^7 viral particles/ml, suspended in saline.

Adenovirus vectors. Replication-incompetent EGFP-actin and red fluorescent (RFP)-actin adenovirus vectors (gift of Dr. James Bamburg, Colorado State University) were kept at concentrations of 3×10^8 plaque-forming units (pfu)/ml in DMEM at −80°C (40). For injections, we used 3×10^5 to 3×10^7 pfu of each adenovirus vector suspended in 0.5 ml of saline solution.

Retrograde Venous Hydrodynamic Injection

Rats were anesthetized by inhaled isoflurane (5% in oxygen, Webster Veterinary Supply, Devens, MA) and then placed on a heating pad to maintain a core body temperature of 37°C. Temperature was monitored using a rectal probe. The abdomen was shaved, cleaned with Betadine Surgical Scrub (Purdue Products, Stamford, CT), and a midline incision was made to expose and isolate the left renal vein. The renal artery and vein were occluded with Micro Serrefine clamps (Fine Science Tools, Foster City, CA).

The vein was then elevated with either 3-0 or 4-0 silk suture thread (Fine Science Tools). At that time 0.5 ml of fluorescent probe or transgene expression vector solution was infused retrograde into the vein (i.e., toward the kidney) over a period of ~5 s, using a 30-gauge stainless steel needle attached to a 1-ml syringe, at the site between the clamp and the kidney (Fig. 1*A*). The needle was removed, and pressure was applied to the injection site using a cotton swab to induce hemostasis. The vascular clamps were removed (the venous clamp was removed before the arterial clamp) to restore renal blood flow. The total clamping period lasted no more than 3 min. After this, the midline incision was closed and the animal was allowed to fully recover.

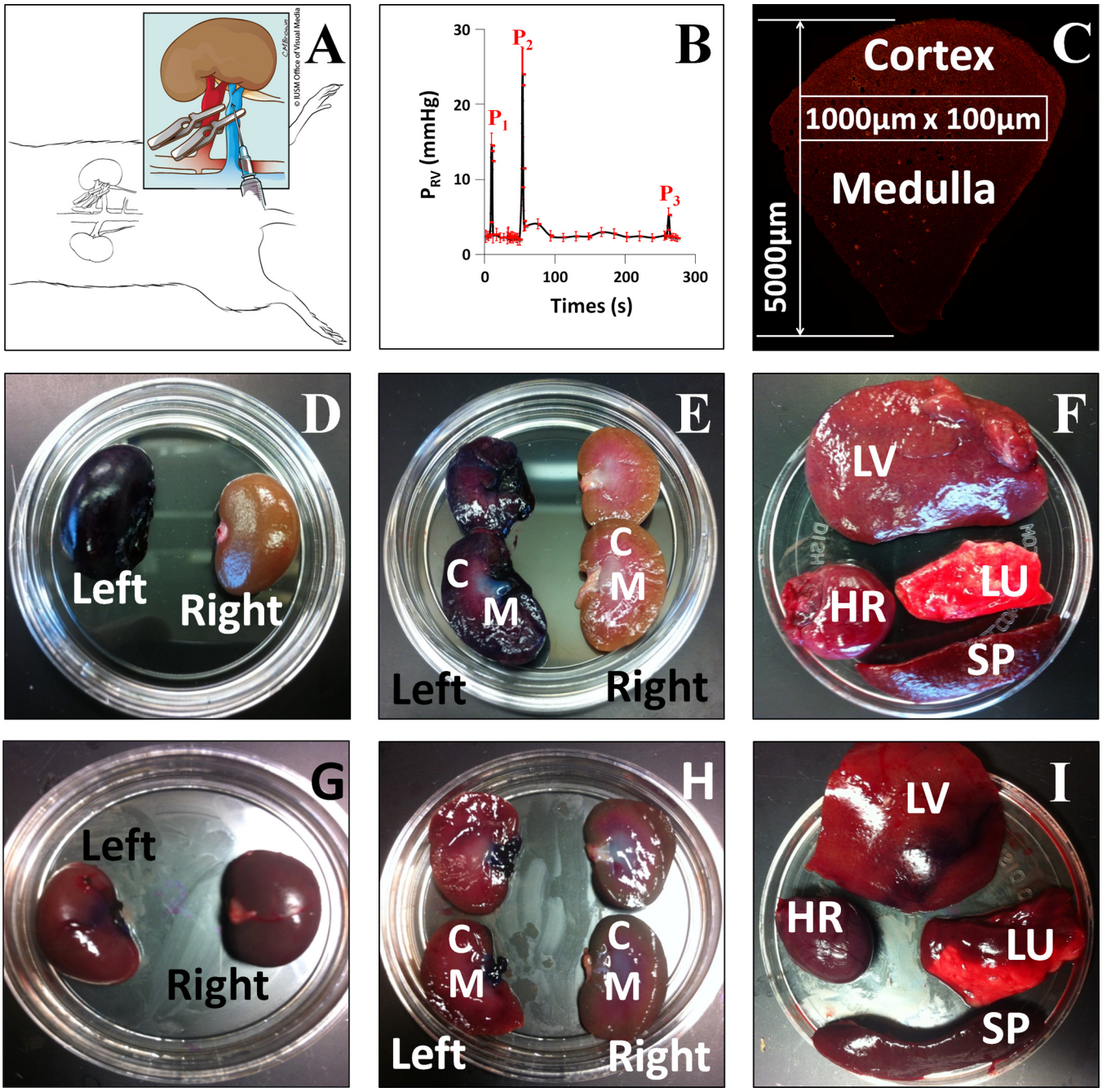

Fig. 1. *A*: schematic illustration of the hydrodynamic injection procedure. Following a laparotomy to expose the left kidney, both the renal artery (red) and vein (blue) were clamped. Reagents to be delivered were injected into the renal vein at a site between the clamp and the kidney. The illustration in Fig. 1*A* was drawn by Chris Brown (IUSM Visual Media). *B*: pressure measured in the renal vein during the hydrodynamic delivery procedure. Pressures were measured using a damped ultrasonic Doppler flowmeter attached to a catheter inserted into the renal vein between the clamp and the kidney. P_1, after both vascular clamps were applied; P_2, hydrodynamic injection; P_3, clamps removed. *C*: schematic illustration of the method used to analyze the efficiency of transfection in different regions of the kidney. The figure shows a montage of Texas Red-phalloidin-labeled sections collected with a ×20 objective and covering a wedge of the kidney extending from the cortex to the hilum. Efficiency of transfection was estimated in 100 × 1,000-µm stripes located at various distances from the cortical surface as illustrated. *D–I*: kidney [*D*, *E*, *G*, and *H*; C, cortex; M, medulla], lung (LU), liver (LV), heart (HR), and spleen (SP; *F* and *I*) recovered from animals following hydrodynamic delivery of toluidine blue dye with (*D–F*) or without (*G–I*) clamping the renal artery and vein. The left kidney was injected in all cases.

Monitoring Vital Signs During Renal Vein Hydrodynamic Retrograde Infusions in Live Rats

We made an incision in the legs of anesthetized rats to expose the femoral arteries. The arteries were isolated with two 3-0 or 4-0 silk loops. Using Micro Serrefine clamps, we clamped off the artery and tied off the loops as well. Each loop was then clamped with a pair of hemostats to stiffen and elevate each artery. We then made a small incision in the femoral artery and inserted a PE-50 tubing catheter into its lumen. The other silk loop was used to anchor the catheter in place. This tubing was attached to a three-way port that was linked to a PowerLab 8/30 data acquisition system (ADInstruments, Colorado Springs, CO) to record temperature, blood pressure, and heart rate.

Fluorescence Microscopy

Intravital and ex vivo two-photon fluorescence microscopy. Each rat was given an intraperitoneal dose of 50 mg/kg pentobarbital sodium and then placed on a heating pad to maintain a core body temperature of 37°C. Once the animal was fully sedated, its left side was shaved and a vertical flank incision was made to externalize the left kidney. The kidney was then positioned inside a glass bottom dish containing saline, which was set above either a ×20 or a ×60 water-immersion objective for imaging (11, 33). Similarly, for ex vivo imaging, sagittal plane sections of kidneys harvested from anesthetized rats were positioned inside the glass bottom dish containing saline.

Fluorescent images were acquired using an Olympus (Center Valley, PA) FV 1000-MPE Microscope equipped with a Spectra-Physics (Santa Clara, CA) MaiTai Deep See laser, with dispersion compensation for two-photon microscopy (11), tuned to 770- to 860-nm excitation wavelengths (33). The system was also equipped with two external detectors for two-photon imaging and dichroic mirrors available for collecting blue, green, and red emissions. The system was mounted on an Olympus IX81 inverted microscope. Bars in all figures are 60 μm.

Jugular vein infusions. Each rat was first anesthetized by inhaled isoflurane (Webster Veterinary Supply), 5% in oxygen, and then given an intraperitoneal injection of ~50 mg/kg of pentobarbital sodium. The rat was placed on a heating pad to maintain its core body temperature of 37°C. Once the animal was fully sedated, its neck was shaved and it was restrained on a heating pad. An incision was made to expose the jugular vein. The vein was isolated with two 3-0 or 4-0 silk loops. The loop closer to the animal's head was tied and clamped with a pair of hemostats to stiffen and elevate this vein. A small incision was then made in the jugular vein to insert a PE-50 tubing catheter into its lumen. The other silk loop was used to anchor the catheter in place. This tubing was attached to a 1-ml syringe containing the solution that would be infused into the vein.

Confocal laser-scanning fluorescence microscopy. Whole kidneys were harvested from live animals directly before euthanasia. These kidneys were immersion fixed with a 4% paraformaldehyde solution. After this, 100- to 200-μm-thick sections were obtained using a vibratome. These sections were then mounted onto glass slides and imaged with the previously described Olympus IX81 inverted microscope in confocal mode.

Estimation of Transgene Delivery Efficiencies

We used two-photon microscopy to analyze the time course and spatial distribution of renal transgene expression. We estimated the transgene delivery efficiency for each vector in vivo using intravital fluorescent two-photon microscopy and in vitro with confocal laser scanning microscopy. Using two-photon microscopy, we determined the efficiency of transgene expression within live superficial cortex segments of several rats across a 28-day period after transgene delivery. We began our measurements 3 days after transgene delivery, having previously determined that this was the point when we reproducibly observed signs of stable transformation and normal renal function.

For these efficiency measurements, we set a threshold signal that was above the highest observed autofluorescence level and distinguished transgene expression from the autofluorescent background. We determined that transgene fluorescence signals had intensities at least double those of autofluorescence signals. Using these thresholds, we then calculated the percentage of nephron cross sections that expressed the reporter transgenes within fields acquired with the ×60 objective. This final percentage (efficiency value) was calculated as the average percentage of transfected (transduced) nephron cross sections within 10 randomly chosen adjacent fields. All values are expressed as means ± SE.

Similarly, our in vitro estimations allowed us to determine the degree of transgene distribution throughout all regions of the cortex and medulla, including those that are presently inaccessible by intravital two-photon microscopy. For these estimations, we first collected a montage of fields using confocal laser-scanning microscopy covering a wedge of the kidney from the renal cortex to the level of the pedicle. Thereafter, we estimated the extent of transformation using the same approach, within 100 × 1,000-μm regions (Fig. 1*C*).

Serum Creatinine Measurements

Creatinine levels were measured in serum samples obtained from rats used in these studies, using the creatinine kinase reagent set (Point Scientific, Canton, MI) in a Beckman Creatinine Analyzer 2 (Beckman Instruments, Brea, CA). Values are reported in milligrams per deciliter (32).

Measurement of Hydrodynamic Injection Parameters

To characterize the hydrodynamic delivery process, we monitored time-dependent pressure profiles during the injection. PE-50 polyethylene catheter tubing (Clay Adams- BectonDickson, Parsippany, NJ) was introduced into the femoral vein and traversed to the level of the bifurcation adjoining the renal vein and inferior vena cava. Both the vena cava and the renal artery were clamped. To monitor pressure, a three-way stopcock was used to connect the infusion line to a fluid-filled pressure transducer, and data were acquired in real time using data-acquisition software (Biopac Systems, Goleta, CA).

RESULTS

Widespread Fluorescent Protein Expression Observed in Various Renal Segments In Vivo, Ex Vivo, and In Vitro

We detected widespread and reproducible expression of a variety of fluorescent protein constructs delivered using the hydrodynamic method. We observed a typical autofluorescent signature and normal morphology in kidneys that were not injected or injected with saline alone (See Figs. 2–8). Following hydrodynamic delivery of plasmid/adenovirus vectors, we observed abundant expression of fluorescent proteins in live kidneys (See Figs. 2–8). The fluorescent protein signals (See Figs. 2–8) were at least double the intensity of the autofluorescence (See Figs. 2–8) and showed characteristic spectral distributions that clearly distinguished them from the endogenous autofluorescence (10, 40). Widespread transgene expression was observed as early as 24 h after hydrodynamic delivery. During the first 36 h after transgene delivery, we occasionally observed cellular debris within tubule lumens. Such tissue damage may have resulted from the hydrodynamic forces produced by the injection or from mild ischemia-reperfusion injury associated with the injection process (26). However, this minimal injury completely subsided after this period,

and at 3 days after the injection the kidneys appeared to be stable without signs of injury. We carried out further studies to confirm that the kidney had not sustained significant injury (see below). We observed no correlation between the appearance of cellular debris and the expression of fluorescent proteins.

Expression of a variety of fluorescent proteins was observed within live proximal and distal tubules (See Figs. 2–6 and Fig. 8); glomeruli (See Fig. 6, *B* and *C*); the supporting interstitium (See Fig. 6*D*); in adipose tissues at the surface of the kidney (See Fig. 6*E*); and the renal capsule (Fig. 6*F*). Fluorescent protein expression was not limited to the superficial cortex, but it was necessary to use confocal microscopy of fixed tissues from injected animals to document expression in deeper regions, which are presently inaccessible to two-photon intravital imaging. High levels of expression were found to extend across the cortex and medulla down to the level of the papilla (See Fig. 7*B*). Furthermore, we noted that a single hydrodynamic injection of a mixture of EGFP-actin and RFP-actin adenovirus vectors generated the simultaneous expression of both fluorescent proteins, sometimes in the same cell, indicating that this method can be used for simultaneous expression of multiple genes.

The morphology of nephron segments expressing fluorescent proteins from plasmid vectors appeared normal. Similarly, injections of adenovirus vectors (3×10^5 pfu) resulted in stable transgene expression with normal tissue morphology. However, injections of higher titers of adenovirus (3×10^6 to 3×10^7 pfu) resulted in fluorescent debris/casts (within tubular lumens) that persisted beyond 3 days after viral delivery, indicating a possible immunological response to higher viral titers. In comparison, following the delivery of baculovirus vectors, areas that expressed fluorescent proteins generally deviated from normal tissue morphology and showed fluorescent protein aggregation (data not shown).

Images obtained from rats that received hydrodynamic injections of plasmids that expressed EGFP-occludin and H2B-tdTomato fluorescent proteins provided clear signs of the expected probe localization and morphology. For instance, EGFP-occludin signals ran between adjacent nuclei as punctate fluorescent bands along regions that would correspond to tight junctions (Fig. 2*J*). Fluorescent histone protein signals from H2B-tdTomato protein expression colocalized with nuclei counterstained with Hoechst (Fig. 2*L*).

Similarly, in images taken from rats injected with plasmids (Fig. 3), or adenovirus vectors containing EGFP-actin (Figs. 4 and 5) and RFP-actin (Fig. 5), there was characteristic labeling of the brush border in proximal tubule cells that expressed these transgenes.

Transgene expression in the glomerulus was investigated primarily in Wistar rats (Fig. 6, *B* and *C*). These rats have superficial glomeruli that are routinely accessible for imaging by two-photon microscopy (33). We also visualized glomerular transgene expression in a Sprague-Dawley rat on the rare occasion that this structure appeared within the range of two-photon imaging in this rat strain. Glomerular morphology was grossly normal in rats that received hydrodynamic saline injections (Fig. 6*A*).

The appearance of fluorescent protein distribution was consistent with expression in podocytes (Fig. 6*B*), but the resolution of our images does not allow us to state this definitively. Similarly, fluorescent protein expression was visualized in S1 segments of proximal tubules and parietal epithelial cells of Bowman's capsule (Fig. 6*C*). Additionally, 150-kDa TRITC-dextran molecules, introduced into the jugular vein of animals that had previously been subject to hydrodynamic plasmid delivery, were characteristically confined to the vasculature (See Fig. 8*D*). This provided further evidence that glomerular structural and functional integrity were maintained following transgene delivery and expression.

Plasmid- and adenovirus-derived fluorescent protein expression was also present in cells within the peritubular interstitium that had morphology similar to either endothelial cells or monocytes (Fig. 6*D*), as well as in cells adjacent to the renal capsule (Fig. 6*F*). Strikingly, no signs of fluorescent protein expression were found in the contralateral kidney (i.e., noninjected kidney) or the other highly vascular organs examined (heart, liver, lung, and spleen).

Hydrodynamic Injections Can Generate Efficient Levels of Transgene Expression in Mammalian Kidneys

We examined tissue sections harvested from rats 3 days after they were treated with plasmids, baculovirus, and adenovirus vectors to gain insight into the efficiency of the hydrodynamic delivery method for each type of vector. For this work, we used confocal laser-scanning microscopy to visualize fluorescent protein expression in kidney sections encompassing the entire depth of the kidney, from the cortical surface to the level of the renal pedicle (Fig. 7*B*). With plasmid or adenovirus vectors, we typically saw that multiple cells (>50%) in a particular tubular cross section simultaneously expressed the fluorescent proteins. However, using baculovirus vectors we frequently observed only single cells expressing the fluorescent proteins.

Baculovirus-based transformation provided the lowest delivery efficiencies, ranging from 10 to 50% of nephron cross sections (Fig. 7*C*). In particular, within the most superficial cortical regions, which would be accessible by intravital two-photon microscopy, there was only a10% efficiency. At depths >500 μm, there was a gradual decrease in fluorescent protein expression in regions that would correspond to the deeper cortex, corticomedullary junction, and medulla.

Much higher levels of fluorescent protein expression were obtained using plasmid and adenovirus vectors (Fig. 7*C*). Using these vectors, 40–86% of nephron segments showed fluorescent protein expression. Within the superficial cortex (<100 μm from the surface), we saw ~78–86% of nephron cross sections expressing fluorescent proteins, explaining the relative ease with which expression was detected in live animals.

The high level of fluorescent protein expression in this superficial region of the cortex permitted us to investigate the level of expression as a function of time by imaging live animals over a 4-wk period. Over this period, the percentages of nephron cross sections expressing fluorescent proteins ranged from 80 to 14% using adenovirus vectors and 61–28% with plasmid vectors (Fig. 7*D*). Thus expression appears to be relatively long-lived with even the rudimentary vectors used in this study.

Nephron Structure and Function Appear Normal After Hydrodynamic Delivery

We looked for evidence of injury following hydrodynamic gene delivery by examining kidney structure and function

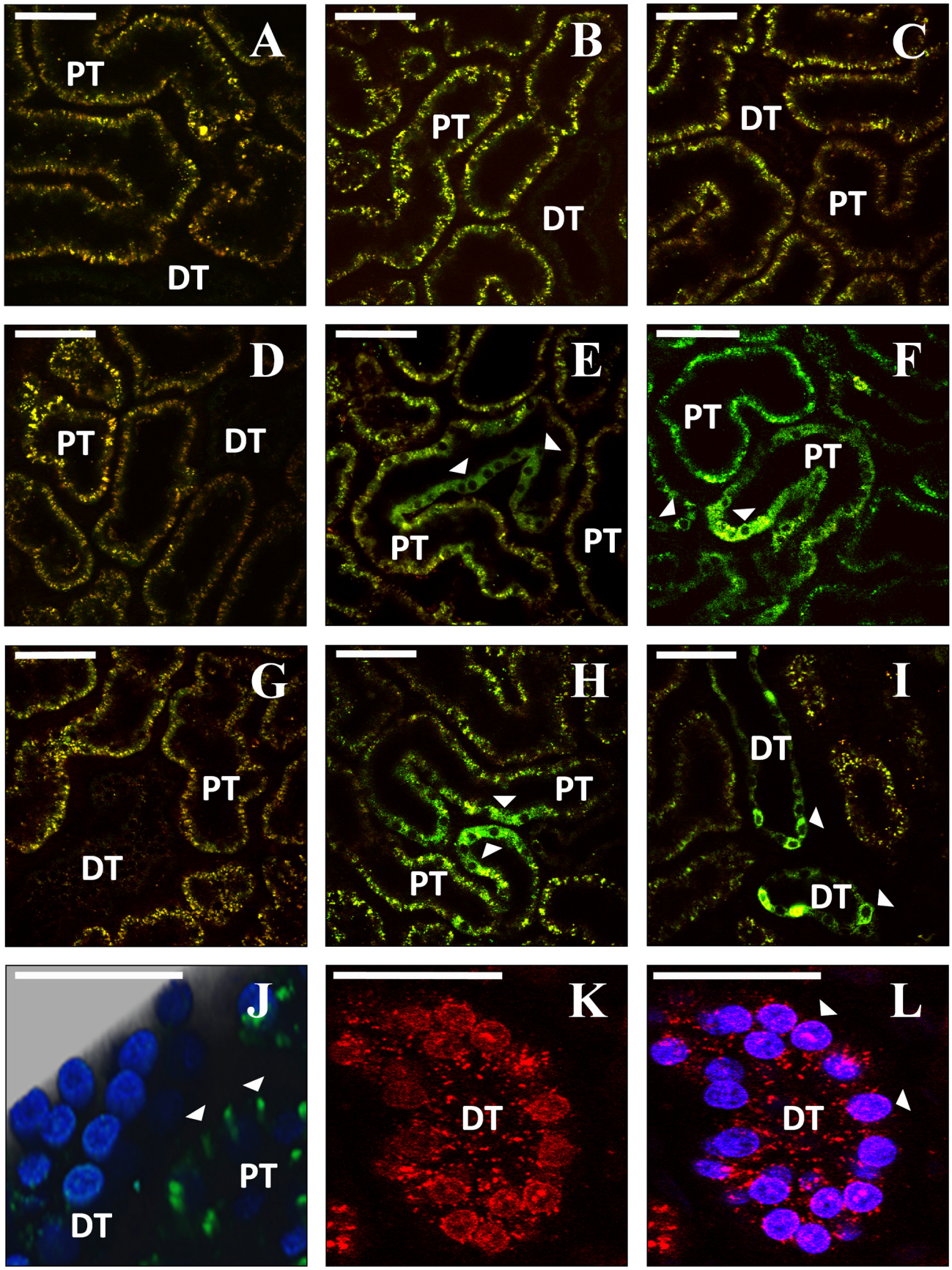

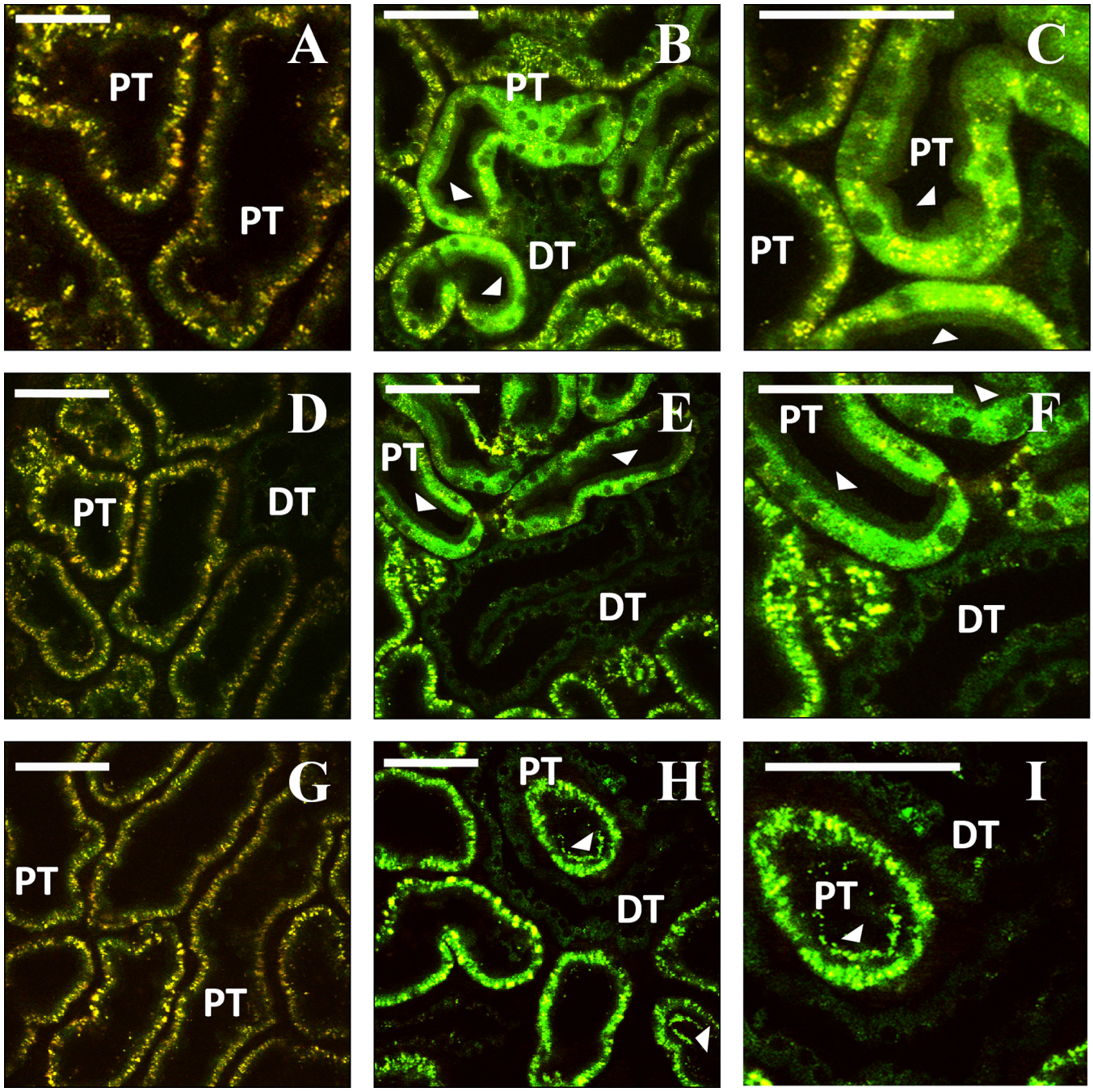

Fig. 3. Time course of expression of EGFP-actin from plasmid vectors. *A*, *D*, and *G*: autofluorescence before injection. *B*, *C*, *E*, *F*, *H*, and *I*: representative field at 2 different magnifications 3 (*B* and *C*), 14 (*E* and *F*), and 28 days (*H* and *I*) after hydrodynamic injection. Arrowheads indicate actin fluorescence in the brush-border microvilli in proximal tubules. Bars = 60 μm.

using several approaches. In animals injected with high-molecular-weight dextrans (150 kDa) via the jugular vein, we observed robust perfusion of the peritubular vasculature and confinement of the dextran by the glomerular filtration barrier. We extended this analysis by simultaneously injecting high (150 kDa) and low (3 kDa) dextrans labeled with TRITC and Cascade blue, respectively, via the jugular vein. This analysis was conducted in rats from 3 to 28 days after they received hydrodynamic

Fig. 2. Intravital imaging shows expression of fluorescent proteins from plasmid vectors. *A*, *D*, and *G*: rat kidneys before hydrodynamic injection. Characteristic autofluorescence signal is detected in both the red and green channels. *B*, *C*, *E*, *F*, *H*, and *I*: 2 representative fields collected from the same animals as in *A*, *D*, or G using the same imaging parameters, 3 days after injection of saline (*B* and *C*), enhanced green fluorescent protein (EGFP) plasmid (*E* and *F*), or EGFP-tubulin plasmid (*H* and *I*). Arrowheads indicate tubular epithelial cells expressing the fluorescent proteins. *J*: 3-dimensional rendering of a volume collected from an animal 3 days after injection of EGFP-occludin plasmid (green). Nuclei are labeled with Hoechst (blue). *K* and *L*: rat kidney 1 day after injection of plasmid encoding tdTomato-histone H2B (red). Nuclei in *L* are labeled with Hoechst (blue). DT, distal tubule; PT, proximal tubule. Bars in all panels = 60 μm.

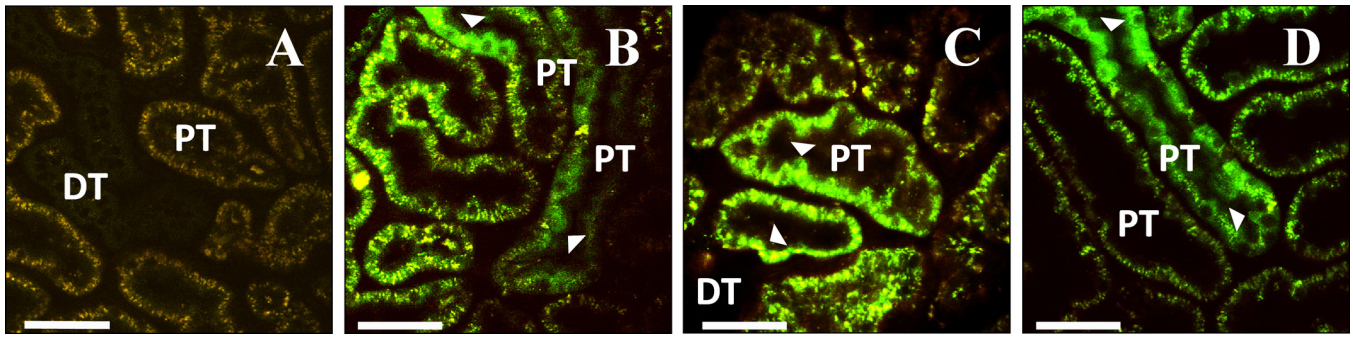

Fig. 4. Expression of EGFP-actin from adenoviral vectors. *A*: autofluorescence before injection. *B*, *C*, and *D*: images collected 3 (*B*), 7 (*C*) or 14 (*D*) days after injection. Arrowheads show expression in proximal tubule epithelial cells. Bars = 60 μm.

transgene injections of plasmids and adenovirus vectors. In all cases, after infusing the dextrans, we observed the rapid appearance of both dextrans in the kidney by intravital two-photon microscopy. Large-molecular-weight dextran molecules were restricted to the vasculature, while low-molecular-weight dextran molecules passed the glomerular filtration barrier, where they gained access to the lumens of proximal tubules, were rapidly endocytosed by proximal tubule epithelial cells, and were concentrated within the distal tubule lumens (Fig. 8*D*). This is consistent with normal nephron function in these animals (3). Importantly, dextrans were taken up equally well by cells expressing fluorescent proteins, indicating that these cells were viable and metabolically active. These data were confirmed by histology studies (Fig. 8, *G* and *H*) that showed normal renal structure within this time frame. However, baculovirus vectors appeared to alter renal structure beyond the 3-day period.

Serum Creatinine Levels and Vital Signs Are Unaffected by the Hydrodynamic Transgene Delivery Process

We monitored creatinine levels in normal rats that received hydrodynamic injections of saline alone or vectors. Creatinine levels in these rats remained within normal baseline levels (0.3–0.5 mg/dl) throughout our measurement period of up to 14 days after hydrodynamic fluid delivery. There was no significant difference in the levels in rats that received isotonic fluid and those that received vectors. Similarly, blood pressure, body temperature, and heart rate were all unaffected by the injection process.

Pressurized Retrograde Venous Injections Provide Widespread Delivery of Exogenous Macromolecules to the Target Kidney Alone

We attempted to clarify the mechanism that permitted highly efficient introduction of exogenous genes into the cells of the kidney. We first investigated the extent of renal uptake that could be attained with solutions injected using this method. For these studies, live rats received hydrodynamic injections of 0.5 ml of toluidine dye solutions. We then harvested whole left and right kidneys, hearts, livers, lungs, and spleens from these rats. Sagittal plane sections of these organs revealed robust distribution of the toluidine dye within the left (injected) kidney, and no traces within the contralateral kidney and the other organs examined when the injection process was performed as described above (Fig. 1, *D–F*).

In comparison, hydrodynamic injections that were conducted without clamping of the renal artery and vein (an approach used unsuccessfully in our early attempts to achieve expression of fluorescent proteins) resulted in minimal uptake of the dye within the target organ (left kidney), and significant levels within the aforementioned offsite and highly vascular organs (Fig. 1, *G–I*).

Hydrodynamic Delivery Facilitates Robust Cellular Internalization of Low-, Intermediate-, and High-Molecular-Weight Exogenous Macromolecules Throughout Live Kidneys

We next investigated whether hydrodynamic infusions could reliably facilitate the cellular uptake of macromolecules in various nephron segments in live animals. For this study, saline

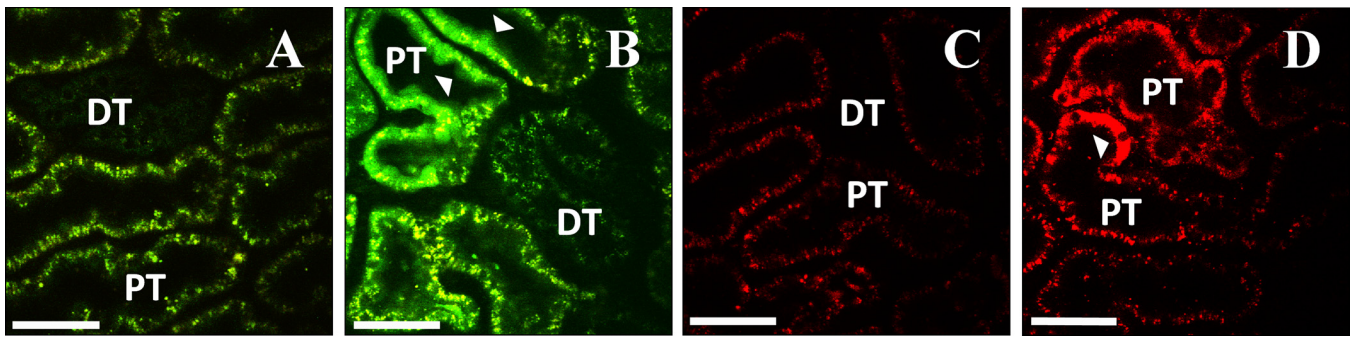

Fig. 5. Comparison of rats injected with EGFP-actin (*B*) or RFP-actin (*D*) adenovirus. Images were collected 3 days after injection. *A* and *C*: images collected before injection. Bars = 60 μm.

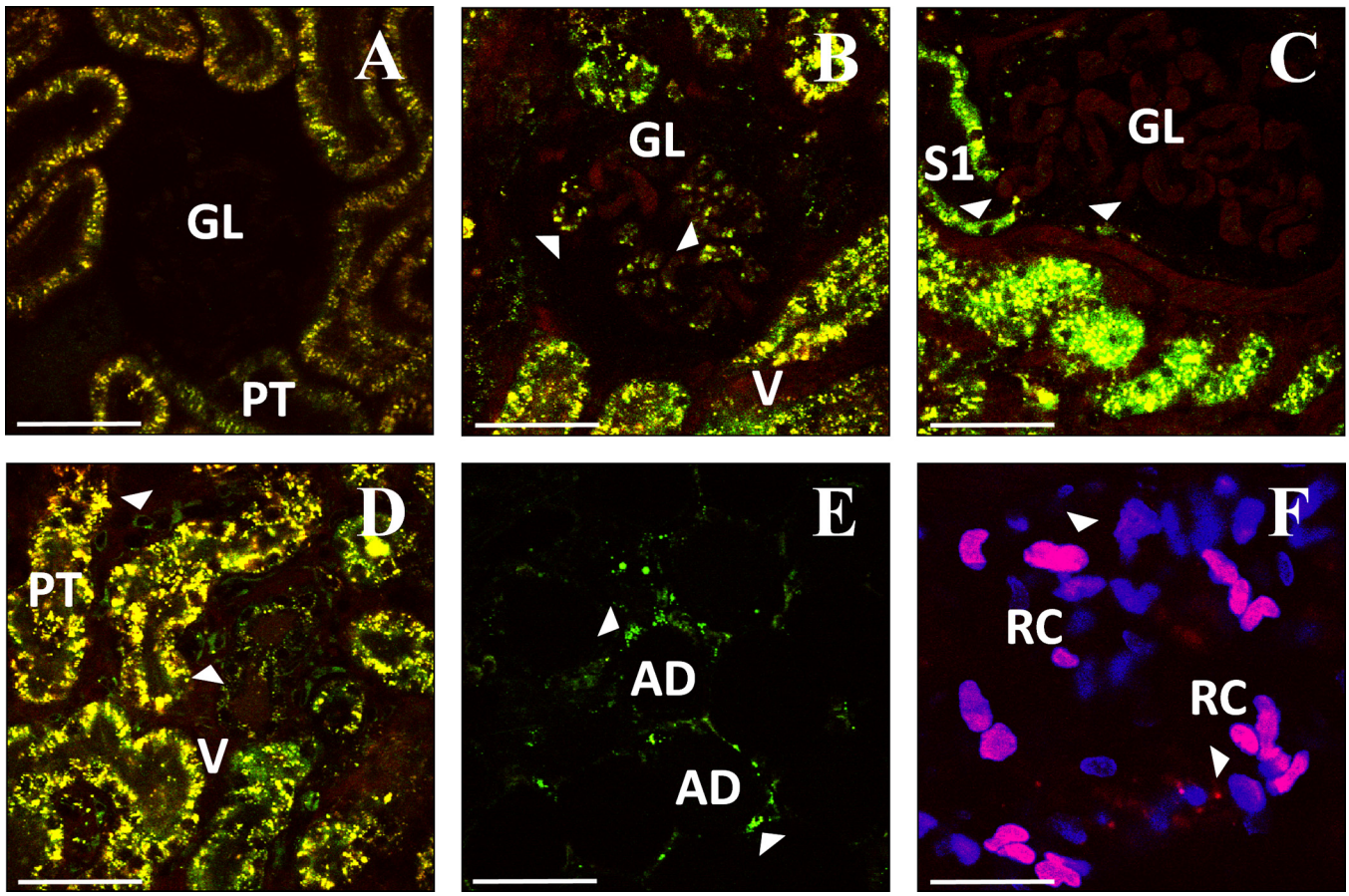

Fig. 6. Expression of EGFP-actin (*B–E*) from plasmid vectors in other kidney cell types (see text). *A*: autofluorescence observed 3 days following saline injection. Expression of EGFP-actin 3 (*B*, *D*, and *E*) or 5 (*C*) days after injection. *F*: expression of td-Tomato-H2B (red) 1 day after injection. Nuclei are labeled with Hoechst (blue). GL, glomerulus; V, microvasculature; S1, S1 segment of proximal tubule; AD, adipocyte in perirenal fat; RC, renal capsular cells. Bars = 60 μm.

solutions containing low (3-kDa Cascade blue and 4-kDa FITC-dextrans)-, intermediate (Texas red-labeled albumin)-, or large (150-kDa FITC- and TRITC-dextran)-molecular-weight compounds were injected into the left renal veins of live rats.

The kidneys were imaged within 20 min after these fine-needle injections. In this case, we observed widespread distribution of the dextrans in vivo (Fig. 8, *A–C*). Remarkably, this pressurized injection facilitated robust and widespread apical

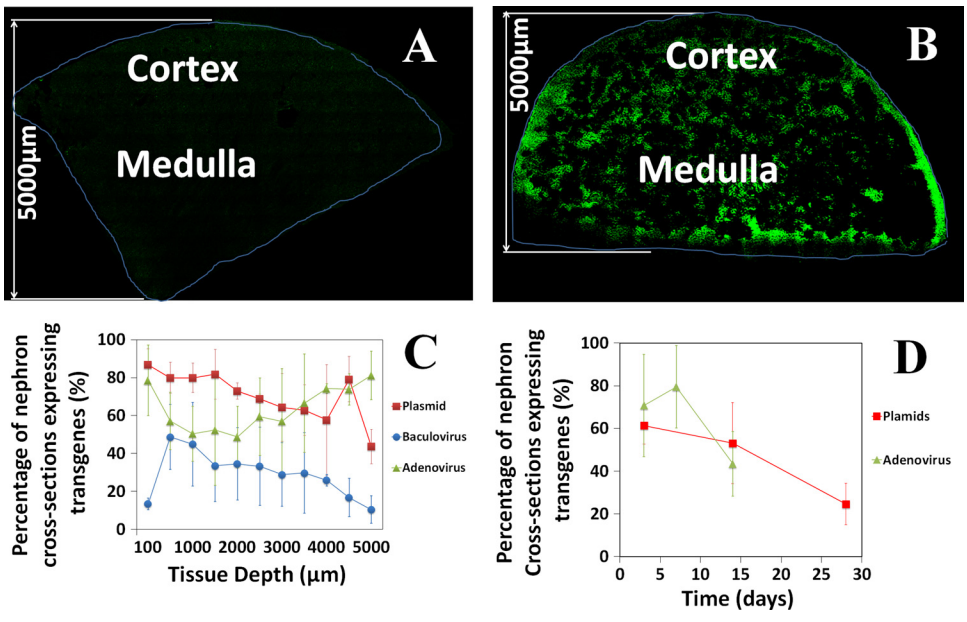

Fig. 7. Quantitative analysis of fluorescent protein expression following hydrodynamic delivery. *A* and *B*: montages collected from fixed kidneys 3 days following injection of saline (*A*) or EGFP-tubulin (*B*). *C*: expression of EGFP-tubulin from plasmid vectors and expression of EGFP-actin from baculovirus or adenoviral vectors at the indicated distances from the cortical surface of the kidney 3 days after injection. *D*: expression of EGFP-actin from plasmid or adenoviral vectors estimated from intravital fields at the indicated times following injection.

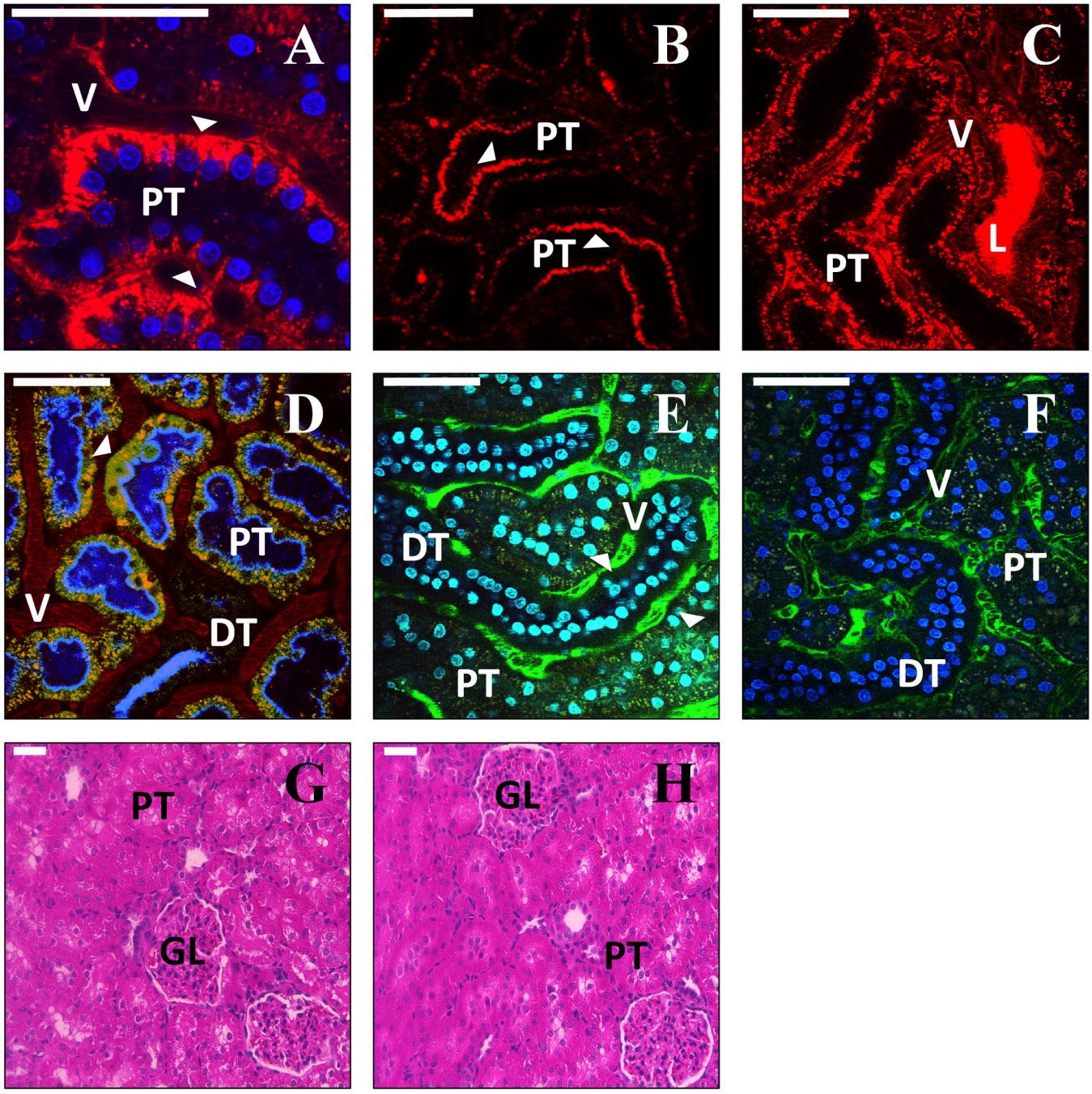

Fig. 8. Assessment of kidney structure and function following hydrodynamic injection and expression of fluorescent proteins. *A–C*: intravital imaging of rat kidneys ~20–30 min following hydrodynamic injection of a 150-kDa TRITC-dextran (red). The dextran is rapidly internalized by proximal tubule epithelial cells (*A*), is visible at the basolateral surface (arrowhead in *A*), and is frequently detected at the apical surface of these cells (arrowheads in *B*). In some instances, bright fluorescence was detected in the lumen of the tubule (*C*). *D*: rat kidney 3 days following injection of EGFP-actin plasmid (green). The kidney was injected with 3-kDa Cascade blue- dextran and 150-kDa TRITC-dextran via the jugular vein ~20 min before imaging. Arrowhead shows abundant endocytosis of dextran in cells that express high levels of the fluorescent protein. *E*: rats were injected with 150-kDa FITC-dextran via the jugular vein 5 min before hydrodynamic injection of saline into the renal vein. FITC-dextran is confined to the vasculature (arrowhead) and is not detected at significant levels in the tubule lumen. *F*: injection of 150-kDa FITC-dextran 20 min following hydrodynamic injection of saline. FITC fluorescence remains confined to the vasculature. *G* and *H*: hematoxylin- and eosin-stained sections from kidneys 3 days after saline (*G*) or EGFP-actin (*H*) injection. L, tubule lumen.

(Fig. 8, *B* and *C*) and basolateral (Fig. 8*A*) distribution and cellular internalization of albumin (data not shown) and large-molecular-weight TRITC-dextran molecules within tubular epithelial cells in a fashion similar to the incorporation of low-molecular-weight dextran molecules into proximal tubular cells (Fig. 8*D*).

We also observed that albumin (data not shown) and large-molecular-weight dextran molecules were uncharacteristically able to access the tubule lumen at high concentrations after being delivered to the kidney via hydrodynamic injections (Fig. 8*C*). Similarly, when 150-kDa molecules were introduced into the bloodstream before hydrodynamic injection of saline,

they were internalized within tubular epithelial cells (Fig. 8*E*). Nevertheless, this atypical access for large-molecular-weight dextran molecules to tubule lumens and tubular epithelial cells was transient and appeared to only occur for molecules present at the time of the hydrodynamic injection process, as 150-kDa dextran molecules infused via the jugular vein ~20–30 min after a hydrodynamic pressurized injection of saline remained confined to the vasculature (Fig. 8*F*).

Critical Parameters Required for Effective Renal Transformation

To characterize critical parameters required for effective transformation, we recorded changes in renal venous pressures generated during the hydrodynamic injection procedure in the renal vein of live rats. From these measurements, we observed that the application and removal of the vascular clamps produced small transient changes in renal pressure. The hydrodynamic fluid delivery produced pressure responses that generally lasted the duration of the infusions. Overall, renal venous pressures increased by up to 25 mmHg (Fig. 1*B*).

DISCUSSION

We have presented a method to rapidly deliver exogenous genes and monitor their expression in live mammalian kidneys. Previous methods described in the literature have produced inconsistent or very limited expression, have required specialized equipment, were technically challenging to perform, or required a tremendous commitment of time and resources in developing new animal strains. Our goals in developing this procedure were that it should be relatively easy for any reasonably skilled animal surgeon to perform, that it should achieve consistent expression from experiment to experiment, that expression should be relatively widespread and reasonably long-lived, and, critically, that there should be minimal injury to the kidney that could complicate subsequent studies. We believe that the procedure described satisfies these criteria in that it provides for *1*) a facile infusion site and vascular manipulations to effect widespread transgene delivery; *2*) a significant degree of vector uptake by several renal cell types; and *3*) limited general injury and vector-derived toxicity.

The innate structural barriers within the kidney pose significant obstacles to the delivery of exogenous genetic material to a variety of renal compartments. Delivery to the tubular epithelial cells, comprising a significant fraction of the renal parenchyma and a key target in many studies, has proved particularly challenging, due to the vascular microanatomy of the organ and the obstacle imposed by the glomerular filtration barrier on access to the tubule lumen. These considerations of tissue architecture probably account for the widely acknowledged failure of approaches such as systemic infusions of viral and plasmid vectors as useful methods for targeting most cells of interest in the kidney.

Since a number of previous reports indicated some success with hydrodynamic delivery, we settled on this approach. Straightforward surgical procedures allow easy access to the renal artery and vein and to the ureter and, in principle, any of the three vessels could provide a feasible access point for hydrodynamic delivery. However, injection into the renal artery proved unsuccessful due to the difficulty in achieving hemostasis without concomitantly inducing an appreciable ischemic injury to the organ. As documented in this report, using the renal vein proved to be remarkably successful in achieving widespread expression of the fluorescent proteins used in our experiments. We have not made sustained efforts at using the ureter as a port of access, but we expect that this, too, could provide a successful route for gene delivery, perhaps being advantageous for certain cell types.

Our studies demonstrate that hydrodynamic forces produced by the injection into the vein allow macromolecules to breach barriers that normally circumscribe their passage through the kidney. High-molecular-weight dextrans could be easily observed in the tubule lumen, as could albumin. An obvious explanation for this observation is that the hydrodynamic forces in the glomerulus that result from the injection somehow breach the glomerular filtration barrier. However, it is hard to conceive that these forces could be a simple increase in the pressure in the glomerular capillaries producing a failure in the barrier, since it is unlikely that delivery at the renal vein could produce an increase in pressure at the glomerulus outside the normal tolerance of the system. We have also not directly observed passage of large macromolecules across the barrier in association with injection, so it is highly plausible that other routes of access to the tubular epithelial cells are possible. These include access to the basal side of the cells via the peritubular capillaries, or possibly a breach of the tight junctions between the cells, which also provides an alternative mechanism to account for their observed appearance in the tubule lumen.

Whatever the mechanism, it is clearly transient, since only large macromolecules present in the vasculature at the time of the injection appeared to be able to access the tubule lumen or transfect the bulk of the cells in the kidney. It is reassuring for the potential utility of this technique that the physical effects of the injection are so short-lived. The effect also appeared to be entirely confined to the kidney whose renal vein was injected, since the contralateral kidney and other highly vascular organs appeared to be completely unaffected. The requirement for proximate delivery of the injection also accounts for the failure of systemic delivery methods to achieve the same results, even those using hydrodynamic delivery.

Our method was particularly successful in achieving transfection of tubular epithelial cells. All segments of the nephron showed expression of the fluorescent proteins, with expression particularly prominent in the proximal and distal convoluted tubules. Other cell types also expressed the fluorescent proteins more sporadically, including cells in the glomerulus and the tubular interstitium. Cell type-specific expression of particular transgenes will require the use of specific promoters, and it is possible that a ureteral delivery method may be more optimal to efficiently target specific cell types.

The vectors used for delivery of the transgenes are clearly a critical parameter in the success of efforts to express exogenous genes in the kidney. The high efficiency of viral infection has made these vectors a favorite of investigators, yet in our studies we achieved essentially equal efficiency using either a plasmid vector or adenovirus. Given the ease of preparation of plasmid vectors and the lesser degree of safety concerns surrounding their use compared with viral vectors, this is clearly a very attractive aspect of this method.

Expression of the fluorescent proteins that were followed over a longer time course was remarkably persistent. There

was only a moderate and progressive decline in the level of expression over a 4-wk period. Since we did not use vectors designed specifically for integration into the host genome, incorporation of the sequences was presumably sporadic and infrequent. However, in the healthy adult kidney the rate of cellular turnover is thought to be relatively slow, and this may account for the fairly long-lived expression observed in our studies.

Baculoviral vectors produced the lowest efficiency of expression in our studies. We assume that the viral particles had the same access to the target cells as did adenoviral vectors, which worked well. We have not investigated the reason for the discrepant behavior of these two systems, which may relate to compatibility with host cell surface molecules necessary for virus entry in the rat system. The baculoviral vectors also seemed to compromise the structure and function of cells that did become infected, as we observed abnormal tubular morphology and fluorescent protein aggregates in cells that did exhibit expression. This contrasted with our observations with the plasmid and adenoviral vectors, where not only was tissue morphology normal in expressing regions but also the cells were clearly viable and metabolically active, as judged by their ability to actively internalize fluorescent dextrans from the tubule lumen.

An absolute imperative in our studies was to devise a method in which long-term injury to the kidney was minimal. Such injury could severely compromise the outcome of future studies. Ischemic injury to the kidney is a serious potential complication, since the procedure involves a brief period of hemostasis. Ischemic injury could clearly be observed in experiments where blood flow to the kidney was halted for more than 5 min, with the formation of debris or casts in the tubule lumen and sluggish microvascular flow in the peritubular capillaries. No such indications of injury were observed in our typical procedure, in which the vessels are clamped for only ~3 min or less. Good technique is thus clearly important, but we believe this should be easy for a practiced animal surgeon to acquire. Investigators using this method should also carefully check for signs of injury using standard methods. Previous work indicated that ischemic injury might facilitate transfection (8), but we did not observe any positive relationship between injury and transfection efficiency.

In the course of these studies, we tried a number of more complex approaches, which have been suggested in the literature to improve the efficiency of transfection in the kidney. These included coupling hydrodynamic injections with ultrasonic pulsation, applied to enhance the disruption of lipid DNA complexes, or combining plasmid DNA with microspheres. None of these augmented procedures enhanced the efficiency of expression compared with hydrodynamic delivery alone, suggesting that the mode of delivery and the route are indeed two of the most critical factors in successful transgene expression.

Widespread, stable, and lengthy transformation recorded in various vascular, tubular, and glomerular cell types accompanied intact renal structure and function. This vast improvement in superficial cellular transformation may be used to facilitate live renal studies that can be directed toward understanding and treating the underlying causes of renal disease.

In conclusion, hydrodynamic-based cell transformation offers an attractive alternative to transgenic models and may be used as a research tool for the study of normal and pathophysiological conditions in live mammals. This method coupled with intravital two-photon microscopy offers near real-time subcellular resolution. Thus hydrodynamic retrograde pressurized fluid delivery may have future clinical utility as a strategy for human genetic therapy.

ACKNOWLEDGMENTS

The authors thank Bruce Molitoris for donating the Wistar rats used in these studies and for many valuable discussions, James Bamburg (Colorado State University) for the adenovirus vectors, Richard Day for the histone plasmids, and Clark Wells [Indiana University School of Medicine (IUSM)] for the occludin plasmids. Also, we thank Randy Brutkiewicz and Andrew Evan at the IUSM, Pei Zhong at Duke University, and Yifei Xing at the Huazhong University of Science and Technology (China) for discussions related to tissue cavitation, retrograde renal transgene delivery, and viral incorporation. We also thank Malgorzatta Kamocka (IUSM), Ruben Sandoval (IUSM), and Shijun Zhang [Department of Biology, Indiana University-Purdue University Indianapolis (IUPUI)] for microscopy support, advice on intravital imaging, and plasmid preparation, respectively. Finally, we thank Angel Anderson and Sylvia Cunningham, School of Liberal Arts, IUPUI, for help with editing early drafts of this manuscript.

GRANTS

This work was supported by the National Institutes of Health (NIH) O'Brien Center for Renal Microscopy and Analysis (P50 4688316; to B. A. Molitoris), and NIH National Institute of Diabetes and Digestive and Kidney Diseases Grants RO1s DK-088934 and DK-053194 (to S. J. Atkinson). All images presented were acquired from systems in the Indiana Center for Biological Microscopy, which was supported by a grant (INGEN) from the Lilly Endowment, Inc.

DISCLOSURES

R. L. Bacallao and S. J. Atkinson have an ownership interest in INphoton LLC.

AUTHOR CONTRIBUTIONS

Author contributions: P.R.C., V.H.G., R.L.B., and S.J.A. provided conception and design of research; P.R.C., G.J.R., and E.C.L. performed experiments; P.R.C., G.J.R., D.P.B., R.L.B., and S.J.A. analyzed data; P.R.C., D.P.B., V.H.G., R.L.B., and S.J.A. interpreted results of experiments; P.R.C. prepared figures; P.R.C., R.L.B., and S.J.A. drafted manuscript; P.R.C., D.P.B., V.H.G., R.L.B., and S.J.A. edited and revised manuscript; P.R.C., G.J.R., E.C.L., D.P.B., V.H.G., R.L.B., and S.J.A. approved final version of manuscript.

REFERENCES

1. **Airenne KJ, Laitinen OH, Mahonen AJ, Yla-Herttuala S.** Transduction of vertebrate cells with recombinant baculovirus. *Cold Spring Harb Protoc* 2009: pdb prot5182, 2009.
2. **Airenne KJ, Makkonen KE, Mahonen AJ, Yla-Herttuala S.** In vivo application and tracking of baculovirus. *Curr Gene Ther* 10: 187–194, 2010.
3. **Ashworth SL, Sandoval RM, Tanner GA, Molitoris BA.** Two-photon microscopy: visualization of kidney dynamics. *Kidney Int* 72: 416–421, 2007.
4. **Basile DP.** Toward an effective gene therapy in renal disease. *Kidney Int* 55: 740–741, 1999.
5. **Bonamassa B, Hai L, Liu D.** Hydrodynamic gene delivery and its applications in pharmaceutical research. *Pharm Res* 28: 694–701, 2011.
6. **Bromberg JS, Boros P, Ding Y, Fu S, Ku T, Qin L, Sung R.** Gene transfer methods for transplantation. *Gene Therapy Methods* 346: 199–224, 2002.
7. **Chang H, Hanawa H, Liu H, Yoshida T, Hayashi M, Watanabe R, Abe S, Toba K, Yoshida K, Elnaggar R, Minagawa S, Okura Y, Kato K, Kodama M, Maruyama H, Miyazaki J, Aizawa Y.** Hydrodynamic-based delivery of an interleukin-22-Ig fusion gene ameliorates experimental autoimmune myocarditis in rats. *J Immunol* 177: 3635–3643, 2006.
8. **Chen S, Agarwal A, Glushakova OY, Jorgensen MS, Salgar SK, Poirier A, Flotte TR, Croker BP, Madsen KM, Atkinson MA, Hauswirth WW, Berns KI, Tisher CC.** Gene delivery in renal tubular

epithelial cells using recombinant adeno-associated viral vectors. *J Am Soc Nephrol* 14: 947–958, 2003.

9. **Decorti G, Malusa N, Furlan G, Candussio L, Klugmann FB.** Endocytosis of gentamicin in a proximal tubular renal cell line. *Life Sci* 65: 1115–1124, 1999.
10. **Dunn KW, Sandoval RM, Kelly KJ, Dagher PC, Tanner GA, Atkinson SJ, Bacallao RL, Molitoris BA.** Functional studies of the kidney of living animals using multicolor two-photon microscopy. *Am J Physiol Cell Physiol* 283: C905–C916, 2002.
11. **Dunn KW, Sutton TA, Sandoval RM.** Live-animal imaging of renal function by multiphoton microscopy. *Curr Protoc Cytom*: Chapter 12: Unit 12.9, 2007.
12. **Edelstein ML, Abedi MR, Wixon J, Edelstein RM.** Gene therapy clinical trials worldwide 1989–2004-an overview. *J Gene Med* 6: 597–602, 2004.
13. **Fisher GH, Orsulic S, Holland E, Hively WP, Li Y, Lewis BC, Williams BO, Varmus HE.** Development of a flexible and specific gene delivery system for production of murine tumor models. *Oncogene* 18: 5253–5260, 1999.
14. **Friedmann T, Roblin R.** Gene therapy for human genetic disease? *Science* 175: 949–955, 1972.
15. **Fujii I, Matsukura M, Ikezawa M, Suzuki S, Shimada T, Miike T.** Adenoviral mediated MyoD gene transfer into fibroblasts: myogenic disease diagnosis. *Brain Dev* 28: 420–425, 2006.
16. **Guy RH, Mehier-Humbert S.** Physical methods for gene transfer: improving the kinetics of gene delivery into cells. *Adv Drug Deliver Rev* 57: 733–753, 2005.
17. **Herweijer H, Wolff JA.** Gene therapy progress and prospects: hydrodynamic gene delivery. *Gene Ther* 14: 99–107, 2007.
18. **Huang S, Kamata T, Takada Y, Ruggeri ZM, Nemerow GR.** Adenovirus interaction with distinct integrins mediates separate events in cell entry and gene delivery to hematopoietic cells. *J Virol* 70: 4502–4508, 1996.
19. **Imai E.** Gene therapy approach in renal disease in the 21st century. *Nephrol Dial Transplant* 16, *Suppl* 5: 26–34, 2001.
20. **Kaunitz JD, Cummins VPS, Mishler D, Nagami GT.** Inhibition of gentamicin uptake into cultured mouse proximal tubule epithelial-cells by L-lysine. *J Clin Pharmacol* 33: 63–69, 1993.
21. **Kelley VR, Sukhatme VP.** Gene transfer in the kidney. *Am J Physiol Renal Physiol* 276: F1–F9, 1999.
22. **Koike H, Tomita N, Azuma H, Taniyama Y, Yamasaki K, Kunugiza Y, Tachibana K, Ogihara T, Morishita R.** An efficient gene transfer method mediated by ultrasound and microbubbles into the kidney. *J Gene Med* 7: 108–116, 2005.
23. **Kost TA, Condreay JP, Jarvis DL.** Baculovirus as versatile vectors for protein expression in insect and mammalian cells. *Nat Biotechnol* 23: 567–575, 2005.
24. **Kukkonen SP, Airenne KJ, Marjomaki V, Laitinen OH, Lehtolainen P, Kankaanpaa P, Mahonen AJ, Raty JK, Nordlund HR, Oker-Blom C, Kulomaa MS, Yla-Herttuala S.** Baculovirus capsid display: a novel tool for transduction imaging. *Mol Ther* 8: 853–862, 2003.
25. **Lecocq M, Andrianaivo F, Warnier MT, Wattiaux-De Coninck S, Wattiaux R, Jadot M.** Uptake by mouse liver and intracellular fate of plasmid DNA after a rapid tail vein injection of a small or a large volume. *J Gene Med* 5: 142–156, 2003.
26. **Li B, Cohen A, Hudson TE, Motlagh D, Amrani DL, Duffield JS.** Mobilized human hematopoietic stem/progenitor cells promote kidney repair after ischemia/reperfusion injury. *Circulation* 121: 2211–2220, 2010.
27. **Lien YH, Lai LW.** Renal gene transfer: nonviral approaches. *Mol Biotechnol* 24: 283–294, 2003.
28. **Liu XF, Shi Y, Zhang JY, Zhuang Y, Jia KR, Mao XH, Guo Y, Liu T, Liu Z, Wu C, Zhang WJ, Zhou WY, Guo G, Zou QM.** Efficient adenovirus-mediated gene transfer to gastric tissue by oral administration. *J Gene Med* 11: 1087–1094, 2009.
29. **Maruyama H, Higuchi N, Kameda S, Miyazaki J, Gejyo F.** Rat liver-targeted naked plasmid DNA transfer by tail vein injection. *Mol Biotechnol* 26: 165–172, 2004.
30. **Maruyama H, Higuchi N, Kameda S, Nakamura G, Shimotori M, Iino N, Higuchi M, Neichi T, Yokoyama S, Kono T, Miyazaki J, Gejyo F.** Sustained transgene expression in rat kidney with naked plasmid DNA and PCR-amplified DNA fragments. *J Biochem* 137: 373–380, 2005.
31. **Maruyama H, Higuchi N, Nishikawa Y, Hirahara H, Iino N, Kameda S, Kawachi H, Yaoita E, Gejyo F, Miyazaki J.** Kidney-targeted naked DNA transfer by retrograde renal vein injection in rats. *Hum Gene Ther* 13: 455–468, 2002.
32. **Molitoris BA, Dagher PC, Sandoval RM, Campos SB, Ashush H, Fridman E, Brafman A, Faerman A, Atkinson SJ, Thompson JD, Kalinski H, Skaliter R, Erlich S, Feinstein E.** siRNA targeted to p53 attenuates ischemic and cisplatin-induced acute kidney injury. *J Am Soc Nephrol* 20: 1754–1764, 2009.
33. **Molitoris BA, Sandoval RM.** Intravital multiphoton microscopy of dynamic renal processes. *Am J Physiol Renal Physiol* 288: F1084–F1089, 2005.
34. **Morral N, O'Neal W, Rice K, Leland M, Kaplan J, Piedra PA, Zhou H, Parks RJ, Velji R, Aguilar-Cordova E, Wadsworth S, Graham FL, Kochanek S, Carey KD, Beaudet AL.** Administration of helper-dependent adenoviral vectors and sequential delivery of different vector serotype for long-term liver-directed gene transfer in baboons. *Proc Natl Acad Sci USA* 96: 12816–12821, 1999.
35. **Moullier P, Friedlander G, Calise D, Ronco P, Perricaudet M, Ferry N.** Adenoviral-mediated gene transfer to renal tubular cells in vivo. *Kidney Int* 45: 1220–1225, 1994.
36. **Newman CM, Bettinger T.** Gene therapy progress and prospects: ultrasound for gene transfer. *Gene Ther* 14: 465–475, 2007.
37. **Suda T, Liu D.** Hydrodynamic gene delivery: its principles and applications. *Mol Ther* 15: 2063–2069, 2007.
38. **Suda T, Suda K, Liu D.** Computer-assisted hydrodynamic gene delivery. *Mol Ther* 16: 1098–1104, 2008.
39. **Tani H, Limn CK, Yap CC, Onishi M, Nozaki M, Nishimune Y, Okahashi N, Kitagawa Y, Watanabe R, Mochizuki R, Moriishi K, Matsuura Y.** In vitro and in vivo gene delivery by recombinant baculoviruses. *J Virol* 77: 9799–9808, 2003.
40. **Tanner GA, Sandoval RM, Molitoris BA, Bamburg JR, Ashworth SL.** Micropuncture gene delivery and intravital two-photon visualization of protein expression in rat kidney. *Am J Physiol Renal Physiol* 289: F638–F643, 2005.
41. **Tanner GA, Sandoval RM, Molitoris BA, Bamburg JR, Ashworth SL.** Micropuncture gene delivery and intravital two-photon visualization of protein expression in rat kidney. *Am J Physiol Renal Physiol* 289: F638–F643, 2005.
42. **Verkman AS, Yang B.** Aquaporin gene delivery to kidney. *Kidney Int* 61: S120–S124, 2002.
43. **von Bonsdorff CH, Fuller SD, Simons K.** Apical and basolateral endocytosis in Madin-Darby canine kidney (MDCK) cells grown on nitrocellulose filters. *EMBO J* 4: 2781–2792, 1985.
44. **Wang G, Zabner J, Deering C, Launspach J, Shao J, Bodner M, Jolly DJ, Davidson BL, McCray PB Jr.** Increasing epithelial junction permeability enhances gene transfer to airway epithelia In vivo. *Am J Respir Cell Mol Biol* 22: 129–138, 2000.
45. **Wells DJ.** Viral and non-viral methods for gene transfer into skeletal muscle. *Curr Opin Drug Disc* 9: 163–168, 2006.
46. **Wu M, Yuan F.** Membrane binding of plasmid DNA and endocytic pathways are involved in electrotransfection of mammalian cells. *PLoS One* 6: e20923, 2011.
47. **Xing Y, Pua EC, Lu X, Zhong P.** Low-amplitude ultrasound enhances hydrodynamic-based gene delivery to rat kidney. *Biochem Biophys Res Commun* 386: 217–222, 2009.
48. **Ye X, Liu X, Li Z, Ray PE.** Efficient gene transfer to rat renal glomeruli with recombinant adenoviral vectors. *Hum Gene Ther* 12: 141–148, 2001.
49. **Zhou T, Kamimura K, Zhang G, Liu D.** Intracellular gene transfer in rats by tail vein injection of plasmid DNA. *AAPS J* 12: 692–698, 2010.
50. **Zhu G, Nicolson AG, Cowley BD, Rosen S, Sukhatme VP.** In vivo adenovirus-mediated gene transfer into normal and cystic rat kidneys. *Gene Ther* 3: 298–304, 1996.